Computers and Concrete, Vol. 3, No. 2/3 (2006) 79-90
DOI: http://dx.doi.org/10.12989/cac.2006.3.2/3.079

Reinforced concrete beams under drop-weight impact loads

Ian M. May† and Yi Chen

Department of Civil Engineering, Heriot-Watt University, Edinburgh EH14 4AS, UK

D. Roger J. Owen, Y. T. Feng and Philip J. Thiele

University of Wales Swansea, Singleton Park, Swansea, SA2 8PP, UK
(Received December 20, 2005, Accepted April 27, 2006)

Abstract. This paper describes the results of an investigation into high mass-low velocity impact behaviour of reinforced concrete beams. Tests have been conducted on fifteen 2.7 m or 1.5 m span beams under drop-weight loads. A high-speed video camera has been used at rates of up to 4,500 frames per second in order to record the crack formation, propagation, particle spallation and scabbing. In some tests the strain in the reinforcement has been recorded using "Durham" strain gauged bars, a technique developed by Scott and Marchand (2000) in which the strain gauges are embedded in the bars, so that the strains in the reinforcement can be recorded without affecting the bond between the concrete and the reinforcement. The impact force acting on the beams has been measured using a load cell placed within the impactor. A high-speed data logging system has been used to record the impact load, strains, accelerations, etc., so that time histories can be obtained. This research has led to the development of computational techniques based on combined continuum/discontinuum methods (finite/discrete element methods) to permit the simulation of impact loaded reinforced concrete beams. The implementation has been within the software package ELFEN (2004). Beams, similar to those tested, have been analysed using ELFEN a good agreement has been obtained for both the load-time histories and the crack patterns.

Keywords: impact testing; drop-weight; RC beams; numerical modelling.

1. Introduction

This investigation was motivated by difficulties encountered by the Authors in providing validated solutions, through computational simulation, for dynamically loaded reinforced concrete structures. The route to confident prediction of the response of such structures, including near ultimate load effects of scabbing, spallation and penetration, has been hampered both by a lack of adequate computational solution procedures and the availability of good quality, comprehensively reported, experimental results.

Limiting attention to low velocity impacts, which, other than ordnance situations, is of most relevance to civil engineering structures, there is a paucity of high quality experimental results. A review of computational and experimental work reported in the field is provided in Bere (2004). The results reported usually take the form of the load/displacement history of the impactor and final

† Professor, Corresponding Author, E-mail: i.m.may@sbe.hw.ac.uk

cracking states of the structure. Partly due to difficulties in historically monitoring quantities under dynamic conditions, little information has been provided regarding the transient development of failure mechanisms.

An experimental and computational investigation programme has been therefore set up. The objectives of the programme were:

(i) To develop computational techniques based on combined continuum/discontinuum methods (finite/discrete element methods) to permit the simulation of impact loaded reinforced concrete structures,

(ii) To validate this methodology by undertaking a controlled series of experimental studies to provide both the necessary input data for computation and results with which to appraise the numerical predictions.

(iii) The initial findings of the programme are described in this paper.

2. Experimental investigation

2.1. Specimens - beams

In total fifteen beams have been tested. Details of the beams are shown in Fig. 1. The beams were nominally 100 mm wide and 200 mm deep. The beams tested were either pin-ended or simply supported at the two ends: the spans between the centres of the supports were 2.7 and 1.5 m for the 3 m and 1.8 m long beams, respectively. The compressive strengths of the concrete cubes, tested at the same time as the beam tests ranged from 34 to 49 N/mm^2. The tensile strength of the concrete was approximately 1.7 N/mm^2, based on the result of the splitting tests of concrete cylinders. High-yield steel reinforcement was used as the main steel, and mild steel round bar for the stirrups. The specifications for the high-yield steel are: Young's modulus = 190 kN/mm^2, 0.2% proof strength = 510 N/mm^2, and ultimate strength = 600 N/mm^2. The tension steel percentage is approximately 0.85%.

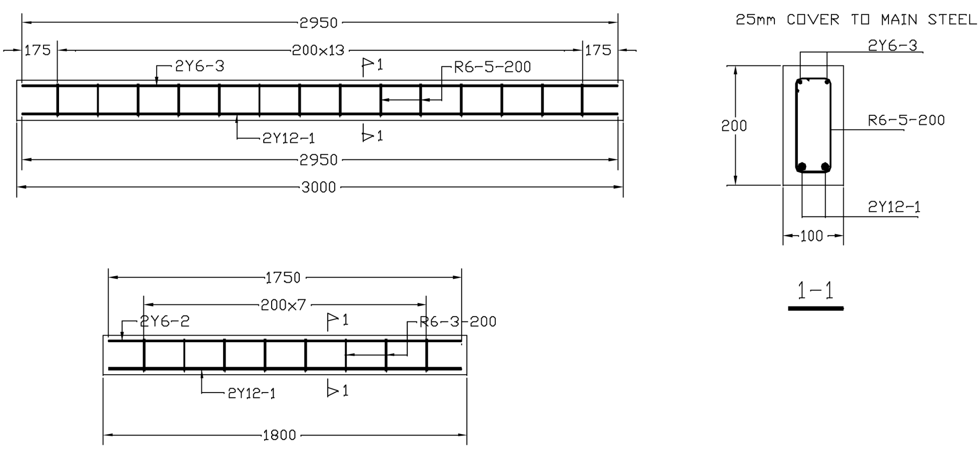

Fig. 1 Details of beams

The main test variables investigated in the beam tests were the shape of the impactor and the type of impact interface. Two steel impactors were used in the tests: a) the first had a spherical surface with a radius of 125 mm and a profile diameter of 90 mm, b) the second had a flat surface and a profile diameter of 100 mm. There were also two types of contact interface used in the beam tests: in the first a 12 mm thick plywood pad was placed on the beam at the impact zone, the second contact interface was to allow the impactor to directly strike the beam.

2.2. Test arrangement

The test facility comprises of a drop-weight system that allows weights of up to 400 kg to be dropped from heights of up to approximately 4 m and guided onto the beam or slab that is being tested. The system has been used to test beams with spans of up to 3.0 m and slabs with sizes of up to 2.5 m square.

In order to provide high quality information about the transient development of the failure mechanisms of the specimens, the following data systems were used:

(i) A high-speed video camera has been used to record the behaviour of beams and slabs in the impact zone using a rate of 4500 frames per second. This enables a transient record of the details of local failure on beams and slabs, such as crack propagation, spallation or scabbing of concrete particles etc, to be obtained.

(ii) The impact force histories have been measured using a load cell fitted beneath the dropping mass and above the impactor. The impactor had mass of 1.4 kg therefore a correction has been made to the load recorded by the load cell to account for the mass of the impactor.

(iii) The acceleration at various locations on the beams has been measured by attaching accelerometers.

(iv) In some of the beam tests, the reinforcement had strain gauges placed inside the bar, namely "Durham" strain gauged bars, a technique developed by Scott and Marchand (2000) so that the strains in the reinforcement can be recorded without affecting the bond between the reinforcement and surrounding concrete.

(v) Two electronic triggers spaced at 40 mm were used to measure the velocity of the dropping mass.

In order to activate the transducers and the high-speed video camera an electronic trigger was used which caused them to start recording simultaneously.

The outputs of the above transducers (load cell, accelerometers and strain gauges) were amplified and then fed in a data logger that can operate at rates of up to 0.5 MHz.

2.3. Test results

Fig. 2 shows the progress of crack propagation and spallation and scabbing formation at the mid span of two of the 2.7 m span beams recorded using the high-speed video camera. The beam shown in Fig. 2(a) was struck by the spherical impactor, through a plywood pad placed on the beam. The beam shown in Fig. 2(b) was struck directly by the flat impactor. For both beams the dropping mass used was 98 kg and the impact velocity was 7.3 m/s. The differences in the behaviour during the the impact event of the two beam tests can be clearly seen. In the first beam, that with the plywood interface, there was less damage due to the energy absorbed in deforming the plywood. Also in the first beam there were mainly shear and flexural cracks occurring in the impact zone, with some

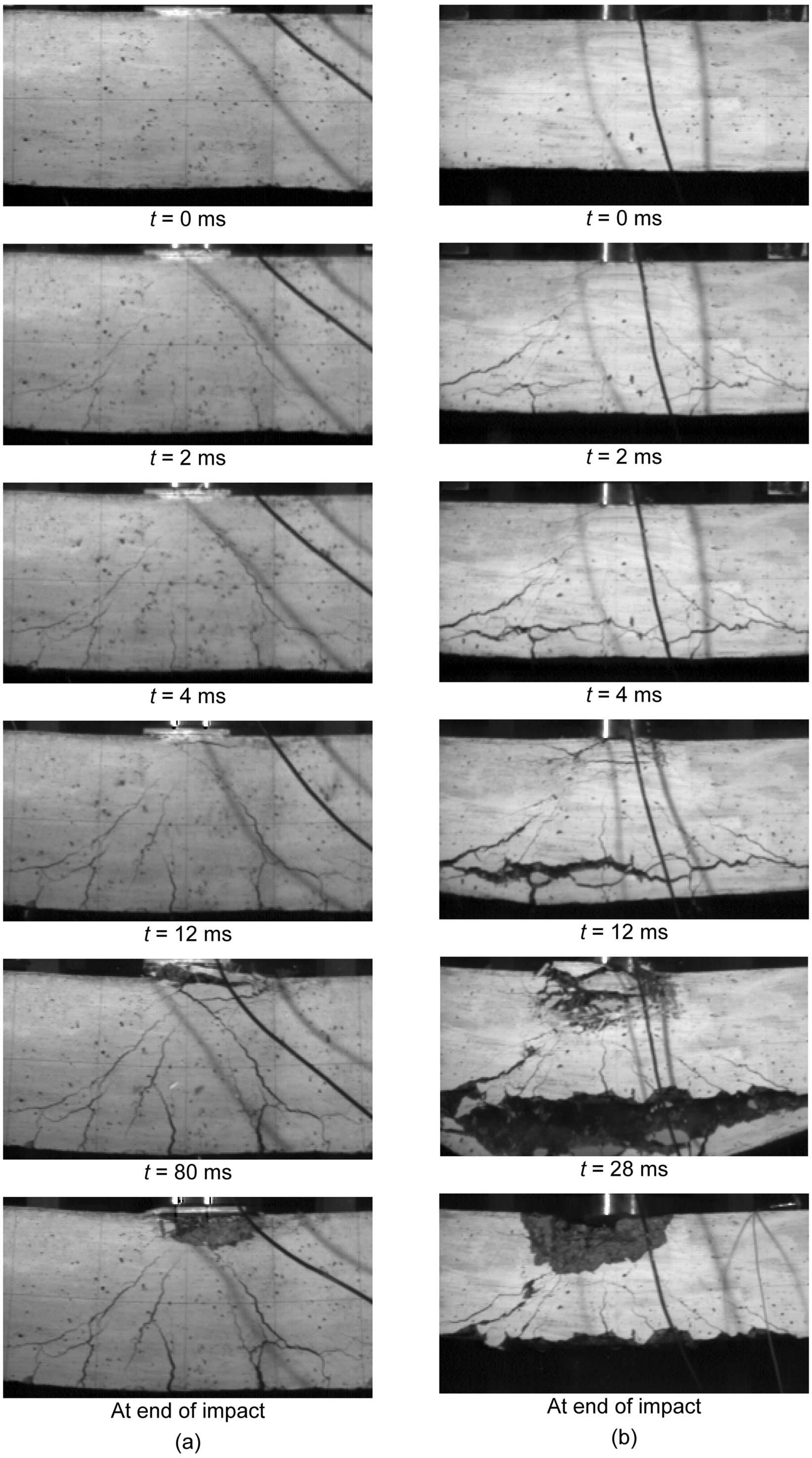

Fig. 2 Beam crack propagation, spallation and scabbing formation

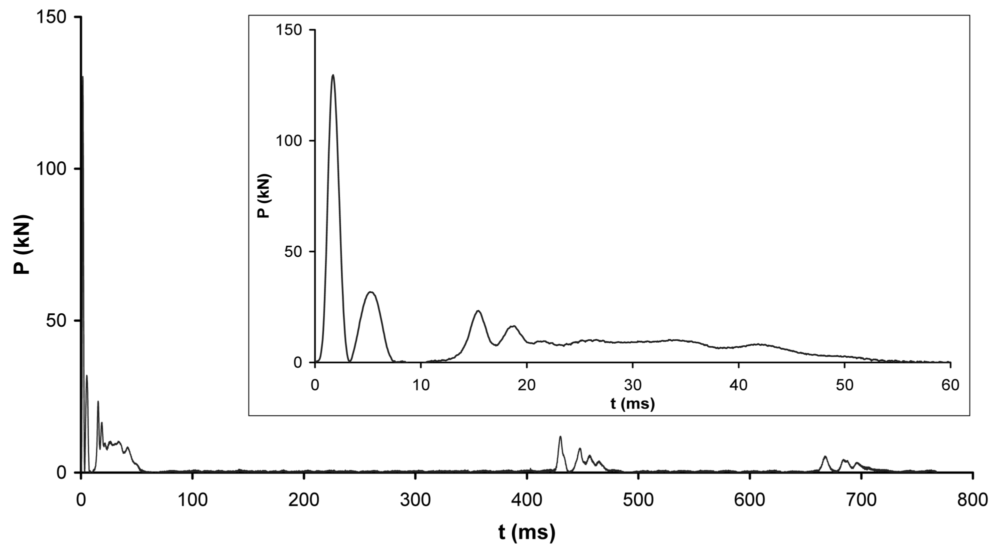

Fig. 3 Impact force time history

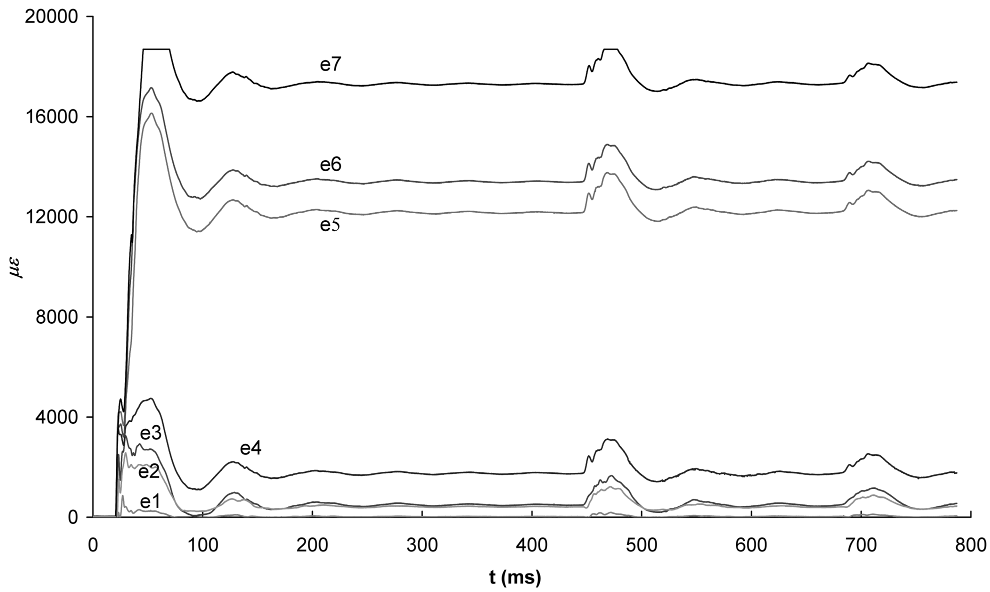

Fig. 4 Reinforcement strain time history

spallation directly beneath the impactor. In the second beam there was similar damage but also extensive scabbing.

The impact force history for the beam in Fig. 2(a) is shown in Fig. 3, where the inset gives a detail of the first 60 ms. From Figs. 2(a) and 3 it can be seen that the impact load increased until cracks started to form after about 2 ms, then it was followed by falling load until about 3.5 ms at which time the beam had a larger velocity than the impactor. There was a very short period of separation between the impactor and the beam. Then the impactor caught up with the beam and

Table 1 Strain gauge locations

Strain gauge no.	e1	e2	e3	e4*	e5	e6	e7*
Distance from mid-span (mm)	900	675	450	100	75	50	100

Note: * Strain gauges e4 and e7 were placed either side of the mid-span of the beam.

they contacted again. This separation at 3.5 ms can be seen from both the load time history and the video (Impact testing). A further separation of about 3 ms duration can be seen after about 8 ms, when the spallation around the impact zone started to occur.

Fig. 4 shows the time histories of typical strains in the reinforcement, readings taken from some of the 25 strain gauges in the "Durham" gauged bar placed in the beam. The locations of the gauges for which readings are shown in Fig. 4 are given in Table 1. It is noted that the three impact events have also been indicated by the sudden changes in the strains.

3. Numerical modelling

From a computational viewpoint, constitutive models are almost invariably based on a continuum formulation, which although permitting the development of crack fields to be simulated in a smeared sense, does not allow discrete fracture paths to be traced and hence precludes the simulation of phenomena such as scabbing and spallation. To capture this behaviour a combined continuum/discrete approach has been used (ELFEN 2004).

The concrete, as a brittle material, is initially represented as a continuum into which cracking is introduced in a smeared sense as the deformation progresses. The onset of fracturing is based on damage mechanics considerations that account for complex stress/strain fields; particularly those involving combinations of compressive and tensile regimes. The approach permits multi-fracturing to occur in the concrete. Key computational issues requiring attention include the fundamental modelling of damage and failure processes through a rigorous continuum description, the treatment of subsequent softening behaviour and the need for mesh objective solutions.

The generally accepted "rotating crack model" is used to simulate crack formation within a continuum description under tensile conditions. In this approach, cracks (in a smeared sense) are initiated in the three directions normal to the principal strains and are presumed to rotate to maintain this orthogonality condition upon further loading. Cracks are initiated when a limiting tensile stress is reached, after which the material follows a softening/damaging response governed by an appropriate relation. Damage models monitor the accumulated damage incurred during the softening process and permit unloading/reloading with a reduced elastic modulus for partially softened material points. It is found to be critical that during the softening process associated with strain localisation during crack formation discretisation objectivity be maintained, in a continuum sense, prior to discrete fracture insertion.

Several options exist to ensure this, recognising that both shear and opening modes of crack extension must be accounted for. Two approaches are investigated, including: 1) An energetic formulation in which the softening slope is related to the fracture energy release rate, G_f, to ensure mesh independent energy dissipation at the local level; and 2) A non-local approach in which averaging of the damage measure in each orthogonal direction is employed to ensure global mesh objectivity. The introduction of rate dependency is also considered as the impact induced strain rate is found to be sufficiently high.

For combined tension/compression regimes, the above model is complemented by a constitutive description based on a Mohr-Coulomb type material model with a limiting compressive cap. The compressive behaviour post-failure is coupled to the tensile softening response and a feature of the model is the ability of the material to independently soften in the three principal stress directions. This constitutive algorithm is capable of predicting fracture for arbitrary tensile/tensile or tensile/compressive stress states.

Following completion of the softening process for an individual smeared crack, a discrete fracture is inserted through the introduction of discrete element concepts. A discrete region is formed from the deformable finite elements describing the original continuum and the constitutive modelling which monitors the onset of fracture as described above. One practical and efficient option is to insert discrete cracks into the continuum on a nodal basis according to a weighted value of a fracture indicator that monitors the damage state of each surrounding element, followed by local element remeshing to provide an adequate element topology. After the insertion of a discrete fracture, the crack surfaces assume a frictional contact response governed by Coulombic representations which will be handled within the combined finite/discrete element environment. A crucial requirement is the maintenance of energy balance during this continuous/discrete transition process.

By modelling the creation of discrete cracks within the original continuum a more realistic representation of this class of problems is obtained, which has the added advantage that the constitutive modelling of the concrete material under non-linear conditions becomes much more tractable.

The reinforcement bars are modelled as beams with an elasto-plastic material property and a perfect bond condition is assumed between the beams and the concrete. The governing dynamic equations of the impact system are numerically solved by employing a central difference based explicit time integration scheme and the time step is selected automatically to ensure the numerical stability of the scheme.

4 Computational example

The numerical example that follows, whilst including all the attributes of the test in terms of geometry, supports etc, does not model exactly the concrete material properties of the test specimens. However, the differences are relatively small and the results can be usefully compared to those obtained from the tests.

4.1. Material properties

4.1.1. Concrete

The concrete specification employed in this model is Grade 50 with a medium size aggregate. The fracture energy, which is dependent on the specifications of the concrete, is 100 N/m. All other linear material properties relevant to the concrete are shown in Table 2.

Table 2 Material properties-concrete

Young's Modulus N/m^2	Poisson's Ratio	Density kg/m^3	Fracture Energy N/m
3e10	0.2	2400	100

Table 3 Strain rate effect on concrete tensile strength

Strain Rate s^{-1}	Tensile Strength N/m^2
0	3.54e6
1	4.60e6
5	8.85e6
20	15.93e6
50	30.09e6
100	44.25e6
1000	56.64e6
10000	60.18e6
100000	60.18e6

Table 4 Material properties-reinforcement

	Young's Modulus N/m^2	Poisson's Ratio	Density kg/m^3	Yield Stress N/m^2	Ultimate Stress N/m^2
Mild	2.1e11	0.29	7800	250e6	280e6
High Yield	2.1e11	0.29	7800	560e6	630e6

Table 5 Material properties-plywood

Young's Modulus N/m^2	Poisson's Ratio	Density kg/m^3
1.5e9	0.3	1500

The tensile strength of the concrete was taken as $0.5\sqrt{f_{cu}}$, where f_{cu} is the concrete compressive strength, and the strain rate effects shown in Table 3 were included.

4.1.2. Steel reinforcement

The reinforcement is high yield bars and mild steel bars for the main reinforcement and stirrups respectively, the material properties are given in Table 4.

The reinforcement is modelled as a non-linear elastic hardening material.

4.1.3. Plywood

The material properties used for the plywood are shown in Table 5. In the tests it was evident that when the impactor and the concrete were separated by plywood packing that could deform plastically and hence absorb some of the energy that would be transferred to the beam otherwise. However, the plywood has been assumed in the analysis to be elastic.

5. General model description

The numerical model of the beam exploits the symmetric properties of the beam and only half of the beam has to be modelled, Fig. 5.

The beam modelled is 3000 mm in length with an effective span of 2700 mm. Its depth and width are 200 mm and 100 mm respectively.

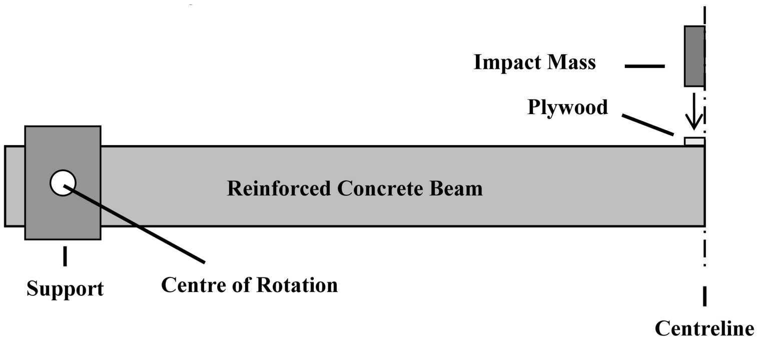

Fig. 5 Schematic diagram of the RC beam model setup

The impactor has a mass of 49 kg, half that in the test because of symmetry, and is projected towards the beam at a constant velocity of 7.3 m/s. The point of contact of the impact mass is at the vertical symmetry line (i.e. at the centre) of the beam.

A layer of plywood, 72 mm long and 12 mm thick is placed on top of the reinforced concrete beam in the zone of contact of the impact mass.

The supports of the beam are placed 150 mm from its outer edges. The beam is pin-ended and hence free to rotate about its neutral axis.

Gravity has been ignored in the numerical simulation as it has an insignificant effect on the results.

A friction coefficient of 0.4 is used in most of the computational models for all contact surfaces. It is later lowered to 0.2 to investigate the effects a decrease in friction in the support. The friction coefficient is of particular importance at the support, as the cylindrical bar holding the support in place is in contact with the outer support and therefore provides some resistance to the beam rotating freely.

Another area where the friction coefficient is of importance is the contact area between the concrete beam and the steel box frame, which is part of the support. It is important that the beam is not completely clamped at this point, because as the beam deforms in the centre, it needs a certain amount of freedom to move in plane with its length in the area of the supports. This is necessary to prevent excessive cracking leading to failure in the region of the supports.

5.1. Finite element mesh

5.1.1. Introduction

The purpose of the 3D model is to establish a more accurate numerical model for the prediction of cracks in the beam. The aim is to improve the insufficient representation of the reinforcement bars, the characteristics of the support and overall representation of the geometry of the beam.

5.1.2. Details of mesh

The mesh used for the concrete, supports and impactor is shown in Fig. 6*a* and the mesh for the reinforcement in Fig. 6*b*. The accurate modelling of the support was found to be an important issue in the analysis.

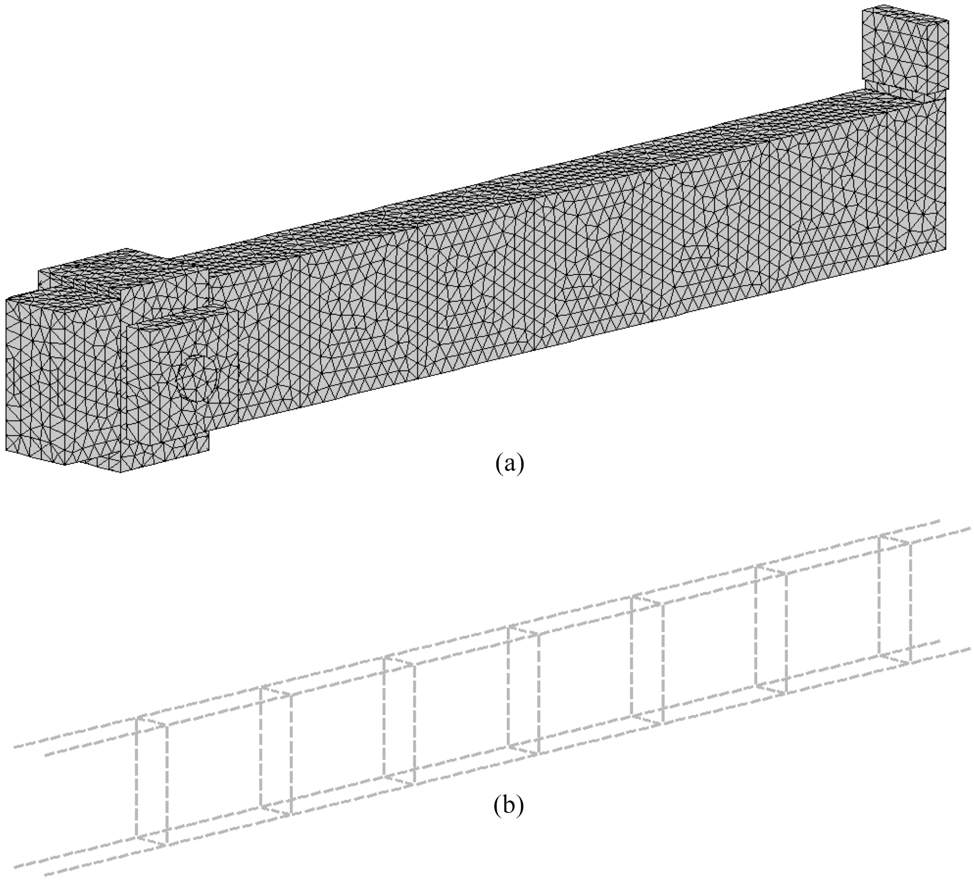

Fig. 6 Details of mesh

5.1.3. Results

The results of the computational model included time history records such as crack path developments and a time-impact force graph as well as reinforcement loading at peak reaction. The wave propagation can also be displayed using the fracture state indicator. Crack patterns can also be displayed. In this discussion only the load time history and final crack patterns will be given.

Fig. 7 shows the numerically obtained time-reaction curve. It can be seen that the impact force increases to a maximum of around 120 kN after 0.5 ms and then starts decreasing. At around 2 ms the impactor loses contact with the beam, which is shown by the impact force being 0 kN. At 2.5 ms the impactor regains contact with the plywood and the beam as the impact force rises up to 20 kN. The impact force then starts to decrease again until it reaches 0 kN after 4 ms. Similar phenomena that were identified in the experimental work.

A physical interpretation of Figs. 3 and 7 leads to the suggestion that the initiation of cracks leads to an abrupt displacement of the beam, hence the beam and the impactor separate for a small period of time. The beam is then slowed down by its own stiffness and the impactor regains contact.

The final crack patterns are compared with the test results in Fig. 8 for the case of plywood packing from which it can be seen that there is good agreement.

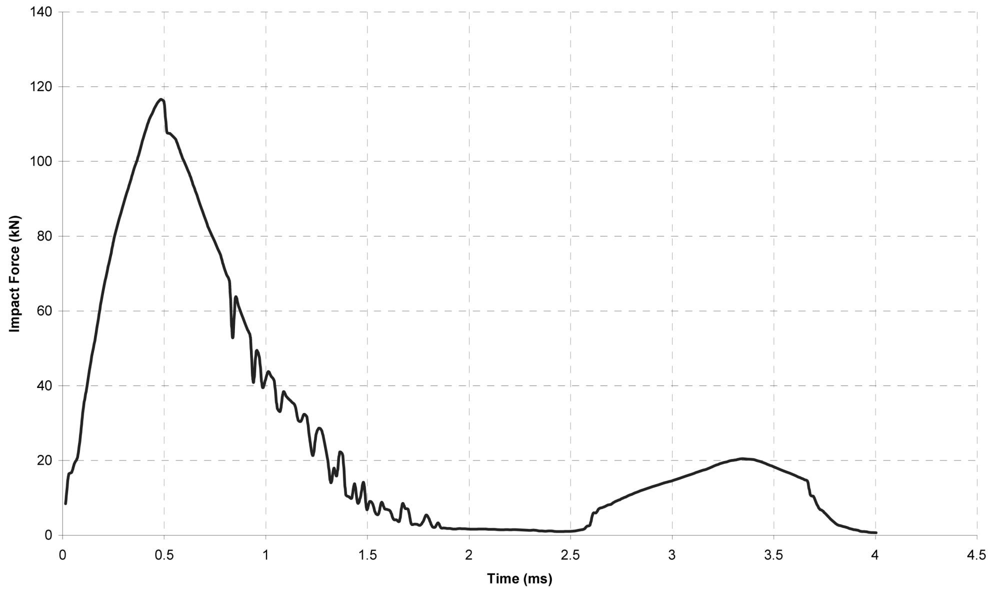

Fig. 7 Load time history

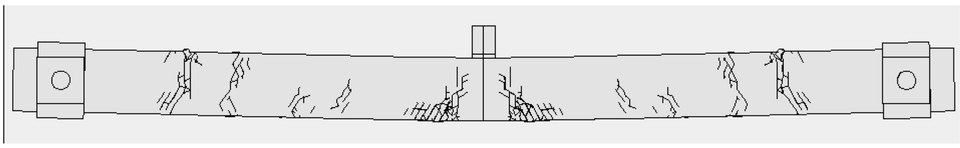

(a) Numerical prediction of crack pattern

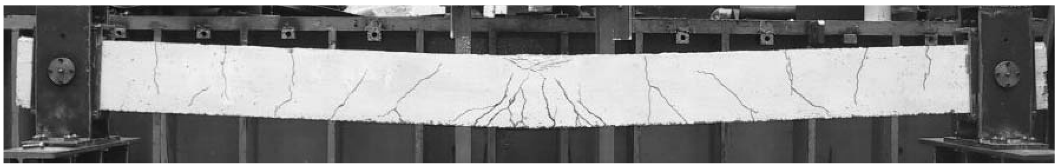

(b) Experimental crack pattern at end of test

Fig. 8 Comparison of tests and numerical model

Further details of the analysis can be found in Thiele (2005).

6. Conclusions

The behaviour of reinforced concrete beams under impact loading has been investigated using high mass-low velocity drop-weight system. The transient formation of local and global failures of beams has been monitored and recorded using several techniques, including high-speed video camera, load cell, "Durham" strain gauged bars and accelerometers. The outputs of the experimental testing have then been used to validate and benchmark the development of the numerical modelling based on FE/DE methods and good agreement has been fouund.

Acknowledgements

The research described in this paper was carried out under grants (GR/R87222 & GR/R87239) awarded by the Engineering and Physical Sciences Research Council (EPSRC).

References

Scott, R. H. and Marchand,, K. A. (2000) "Measurement of reinforcement strains caused by blast loading", *Strain*, **36**(4), 161-164.

ELFEN (2004) 2.8, Rockfield Software Ltd., Swansea, UK.

Bere, A. T. (2004) "Computational modelling of large-scale reinforced concrete structures subject to dynamic loading", PhD Thesis, Univ. of Wales Swansea.

Impact testing. [Online] (2005) Available at: http://www.sbe.hw.ac.uk/research/structural/impact_test/index.htm [August 10].

Thiele, P. J. (2005) "Behaviour of reinforced concrete beams under low-velocity impact loads", MRes Thesis, University of Wales Swansea.

NB